www.czasopisma.pan.pl PAN POLSKA AKADEMIA NAUK www.journals.pan.pl

Arch. Metall. Mater. **70** (2025), 4, 1553-1564

DOI: https://doi.org/10.24425/amm.2025.156235

BILGEHAN ŞAHIN[1], ATILLA EVCIN[2*]

ASSESSMENT OF MECHANICAL AND BALLISTIC PERFORMANCE OF ARAMID-BASED COMPOSITE MATERIALS REINFORCED WITH GRAPHENE

The main purpose of this research is the impact of graphene nanoparticle reinforcement on ballistic protection of composites and to investigate the ballistic and mechanical properties of these products. In this context nanocomposite ballistic plates were obtained by reinforcing different amounts of graphene to aramid-based composite plates after some processes. To characterize the graphene, several analyses were performed. Characteristic peaks were obtained by performing FTIR (Fourier Transform InFrared). Scanning Electron Microscopy (SEM) and Raman analyzes on graphene nanoplatelets used in the experimental study. Ballistic plates reinforced with graphene nanoplatelets and non-reinforced plates were subjected to shooting tests in the ballistic test laboratory in accordance with the NIJ (National Institute of Justice) standard and the test results were compared. As a result of the shooting tests, successful results were not achieved with ballistic plates reinforced with graphene and epoxy resin, except for one plate. This outcome was attributed to the negative impact of epoxy resin on the flexibility and energy absorption properties of the aramid layers. From a mechanical properties perspective, it was observed that the ultimate tensile strength of the samples with 0.5% and 1% by weight graphene increased.

Keywords: Graphene; Nanomaterial; Composite; Ballistic Test; Tensile Strength

1. Introduction

In an environment where technology is developing at a rapid pace, nanomaterials with extraordinary properties are used across various industries, including space, aviation, automotive, energy, medicine, biology, defense industry. When going from macro dimension to nano dimension, materials; the power/weight ratio, conductivity, optical and magnetic properties vary considerably and provide added value in the final material design.

The defense industry has also become one of the areas where nanomaterials are widely used. In this context, the design of ballistic protective armor has gained importance alongside the advancement of weapon technology. In recent years, the development of nanoparticle reinforced composite materials has been the focus of attention. Advanced technology nanocomposite materials can be produced by reinforcing carbon nanostructures (graphene, carbon nanotube, etc.) into composite materials.

Nanotechnology is the design and development of innovative, interdisciplinary scientific approaches, and the design of materials and devices at the molecular level and at the nanometer scale, that is, the size of at least one dimension is between 1 and 100 nanometers [1]. As stated in this definition, nanotechnology has the potential to design new materials and devices at the nanometer scale.

Nanomaterials make stronger and lighter armor, reduce maintenance costs and improve the performance of kinetic weapons [2]. It is believed that nanomaterials used in armor production can improve features such as lightness, strength, ballistic protection, and ease of use. In this context, it is predicted that nanomaterials can be added to polymer-based fabrics used in the production of ballistic protective materials, adding functionality to the forementioned products and improving the physical, mechanical and ballistic properties of the final products to be formed.

The aim of body armor research is to manage the conflicting objectives of armor production such as low cost, light weight, comfortable systems, and superior ballistic protective performance [3]. These researches have been going on since World War II and studies on the ballistic effect of body armor materials have increasingly continued.

Nanomaterials have only recently been incorporated into composite armors. While carbon nanotubes provide a high amount

[1] AFYON KOCATEPE UNIVERSITY, INSTITUTE OF SCIENCE, DEPARTMENT OF MATERIAL SCIENCES AND ENGINEERING, AFYONKARAHISAR, TURKEY
[2] AFYON KOCATEPE UNIVERSITY, FACULTY OF ENGINEERING, DEPARTMENT OF MATERIAL SCIENCES AND ENGINEERING, AFYONKARAHISAR, TURKEY
* Corresponding author: evcin@aku.edu.tr

of strength and stiffness to the composites, inorganic fullerenes increase the energy absorption capacity of the composites [4]. If cost-effective, these nanomaterials are expected to reduce the weight of ballistic composites and increase their strength.

Nanotechnology has great potential in the field of protective clothing due to the excellent physical, chemical, mechanical and electrical properties of nanomaterials. Thiragavati et al. [5] explored the application of nanotechnology in sensors, energy storage, conductive, and anti-fouling fabrics, and the production of lightweight and comfortable protective clothing for military personnel. The research focused on microfibers and nanofibers. They found that protective clothing made of these fibers and their composites can provide higher performance, comfort and longer material life, while requiring less weight, size, maintenance and cost.

1.1. Body Armor and Ballistic Fibers

Advanced body armor can be classified into two class based on the materials used: hard armor and soft armor. Generally speaking, hard armor provides a higher level of protection than soft armor. Soft armor is favored for its flexibility, lightness, and comfort. Hard armor is made of rigid materials such as ceramics, reinforced plastics, plates, and composites. Soft armor consists of multiple layers of high-performance ballistic fiber materials [6]. These fibers are made into advanced fabrics or other textures or similar structures that can be sewn together to make vests and other soft wearable garments. In general, soft body armor for bullet protection is made of multiple layers of interwoven textures sewn together. Today, they consist of non-woven laminates, unidirectional sheets, and combinations of woven or non-woven laminates. In this experimental process, graphene-reinforced aramid fabric laminates were used to obtain soft armor plates.

For ballistic protection, fibers must exhibit low density, exceptional strength, and high energy absorption capacity. A material's ballistic effectiveness is determined by its ability to absorb impact energy at the point of contact and spread it across the entire structure. Critical factors influencing the protective capability of textile fibers include their tensile strength, elongation characteristics, and the speed at which sound propagates through the material (known as the velocity of sound) [7].

Aramid fibers, one of the ballistic fibers, are a high strength polymer with exceptional strength/weight properties. Aramid fibers are known for their stiffness and resistance to penetration. Due to their high strength and durability, they are used in the production of materials that require perforation-proof properties. Aramid has started to replace nylon in light ballistic armor since the 1960s.

Aramids are divided into two groups, meta-aramid and para-aramid, according to their structure and properties. Meta-Aramids have high resistance to heat, are suitable for flame retardant clothes. Types of aramid fabrics used in ballistic applications are para-aramid fibers that we deal in that research. The most well-known types of fabrics are Kevlar®, Twaron® and Technora® which are named acoording to their commercial producer [8].

1.2. Graphene and Its Importance for Composite and Armor

Since scientists Geim and Novoselov studied single-layer graphene in 2004 [10], this atomically thin carbon layer has received increasing attention in materials research. Graphene has many excellent properties, such as large surface area, excellent thermal conductivity, extremely high elastic modulus, and high electron mobility at room temperature. These properties make graphene a great complementary material for nanocomposites.

As observed in other nanoparticles, the properties of the nanocomposite material are maximized when the graphene particles are homogeneously dispersed into the matrix. Because the impact effect is transferred to the integrated polymer and nanoparticle layer [11]. In this way, the homogeneous distribution and strong interaction between the graphene and the matrix improves the performance of the graphene nanocomposite material [12]. Distributing the impact effect on the ballistic panel on the surface and layers is one of the desired properties in terms of ballistic strength. Therefore, dispersion and the strong interaction between graphene and matrices are key for the performance of graphene nanocomposites.

Instead of the aramid fabric-based body armor, Graphene based composites came into the picture. Recently, for instance Lee et al. Described that in their work, the specific infiltration energy of the microparticles were an order of magnitude higher than that macroscopic steel, with multilayer graphene ten times more [13].

Graphene oxide (GO) is a graphene derivative obtained as a result of the oxidation of graphite. Since it contains epoxy, hydroxyl, carbonyl and carboxyl groups in its structure, it gains the opportunity to bond with other molecules. Peirera et al. [14] demonstrated that the incorporation of GO into an epoxy matrix significantly enhances the ballistic properties when combined with ramie fabric. The energy absorption capacity of ramie fabric reinforced with GO epoxy nanocomposites is 23.4% higher compared to Kevlar alone. These GO-reinforced ramie fabric nanocomposites emerge as a promising material for the second layer in ceramic-fronted multi-layered ballistic armor designed for personal protection.

1.3. Ballistic Test Standards

Ballistic protection is based on the principle of reducing the energy transferred from a projectile. There are many different standards used to determine the protection status of ballistic protective materials around the world, and these standards are shown in TABLE 1 [15].

The widely used standards among these standards are NIJ (National Institute of Justice) standards. These standards are set by the US Department of Justice's National Institute of Justice.

TABLE 1

Ballistic Test Standards [15]

Type of Standard	Name of Standard
TS 11164	Ballistic Protective Body Armor
TS 13349	Military Armors – V50 ballistic speed experiment
MIL-A-46103 C	Light Weight, Ceramic Faced Composite Armor Procedure Requirements
MIL-B-44053	A Fragmentation Protective Body Armor, Vest Ground Troops
MIL-STD-662 F	Ballistic Test for Armor
NIJ-STD-0101.04	Ballistic Resistance of Personal Body Armor
NIJ-STD-0101.06	Ballistic Resistance of Personal Body Armor
NIJ-STD-0108.04	Ballistic Resistance of Protective Materials
STANAG 2920	Ballistic Test Method for Personal Armor
UK/SC/4697	The Ballistic Testing of Fragment Protective Personal Armors
UL 752 PPAA STD-1989-05	Ballistic Resistance Equipment Ballistic Resistance of Personal Body

The purpose of these standards is to specify minimum performance requirements and test methods for the ballistic resistance of personal body armor intended to protect the body against gunfire.

The NIJ-STD-0101.04 standard is one of the most common NIJ standards used to test the protection of body armor. The test criteria of this standard are shown in TABLE 2 [16]. In this table, values such as bullet diameter, weight, speed, amount of shot, maximum amount of deformation on the target, which should be used for testing at different protection levels, are included.

Today, the protection level of ballistic protective equipment is determined by the level of threat that may be exposed [17]. The ideal level of protection for ballistic helmets is IIIA, which provides protection against pistol and machine gun bullets. However, as the level of protection increases, it is inevitable that the weight will increase. Therefore, this will not be ergonomic and usable for the helmets, as the higher protection level will bring more weight.

Although body armor is used to prevent small arms bullets from penetrating the body, sometimes bullets can cause recessed deformations and life-threatening injuries can occur. Impact can cause blunt trauma to the back of the armor as shown in Fig. 1. Serious injury to tissues, skeletal structures and organs can occur and can be fatal. Blunt trauma may not be instantaneous, but due to the propagation of ballistic waves throughout the body, it may manifest itself later and damage distant organs [18].

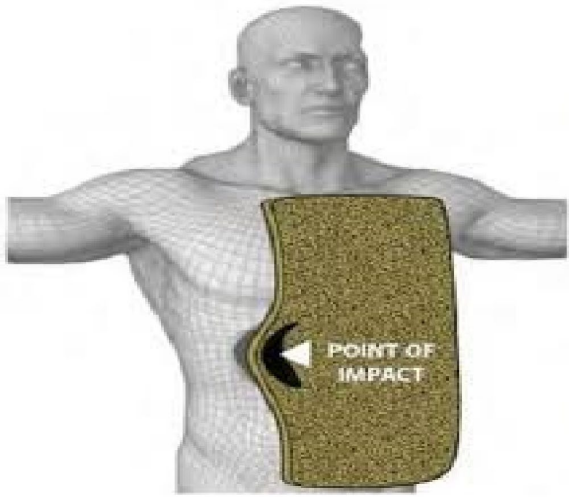

Fig. 1. Blunt trauma [18]

1.4. Ballistic Protection Mechanism

The working principles of ballistic protective materials are generally divided into two categories: absorption of impact energy and redistribution of impact energy. A shielding material must absorb a bullet's energy before it can fully penetrate the material. Energy absorption is obtained by stretching, compressing or destroying the material. In other words, the working principle

TABLE 2

Ballistic Test Standards [16]

Level of Protection	Type of Bullet	Speed of Bullet (m/s)	Weight of Bullet (g)	Distance to Target (m)	Max. Amount of Deformation (mm)
I	0.38 special RN 0.22 kalibre	329±10 322±10	10.2 2.6	5	44
IIA	0.357 mag, JSP 9 mm FMJ	341±10 322±10	10.2 8.0	5	44
II	0.44 mag, JW 9 mm FMJ	436±10 367±10	10.2 8.0	5	44
IIIA	0.44 mag, SWC 9mm FMJ	436± 10 436± 10	15.55 8.0	5	44
III	7.62 mm FMJ	838± 10	9.7	15	44
IV	36-60 AP	869± 10	10.8	15	44

of body armor is based on the rapid conversion and dissipation of kinetic energy from a striking bullet into tension energy within the ballistic body armor [19].

The main parameters affecting the distribution of impact energy are; the tensile strength of fabrics and yarns, fabric structures and the number of fabric layers. When a bullet hits a fabric or several layers of fabric, two waves emanate from the point of impact on the outer surface, longitudinal and transverse waves. As seen in Fig. 2, the longitudinal wave moves in the plane of the fabric and the transverse wave spreads perpendicularly to the fabric. The absorption capacity of these waves by the layers of the fabric is an important factor that determines the ballistic protective performance.

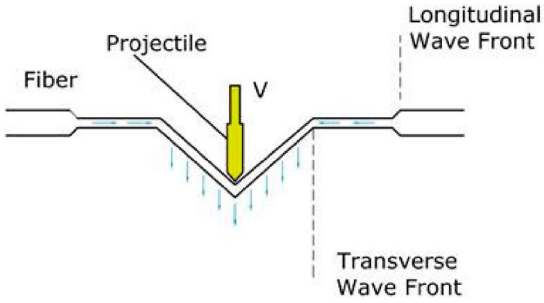

Fig. 2. Longitudinal and transverse waves

2. Materials and method

In this study; the main goal is to manufacture a soft body armor product in nanocomposite structure by reinforcing graphene nano powder as a nanomaterial and to evaluate and compare this armor product's ballistic and mechanical properties.

2.1. Materials

In this study, ballistic test plates, were designed according to small plate sizes. The dimensions of the plates were 250 mm × 250 mm. Different precursors were used in fabricating the plates: Kevlar® (Dupont), Grafen (Nanografi, Türkiye), and epoxy resin (Verpol, Türkiye). Their technical specifications are given in TABLES 3-5 respectively. Aramid fabric type is 100% aramid. Fabric texture type is 1/1 (one by one) plain. One side of the fabric is coated with colorless phenolic based polyvinyl butyral (PVB) resin. The unit area mass of the PVB resin coated fabric is at most 490 g/m^2. The unit area mass of the coating is 55 g/m^2. The yarn density of the fabric is at least 60 pieces/10 cm in weft and warp.

2.2. Production of Ballistic Plates

For the production of ballistic test plates, aramid fabric, which is the main armor fabric, is cut in the Automatic Fabric Spreading and Cutting Machine that is shown in Fig. 3. The aramid fabric sections cut in the desired dimensions are stacked on top of each other in the desired number of layers.

The second step for plate production is the application of the graphene and epoxy resin mixture to the aramid fabric layers by hand lay-up technique. Aramid fabric layers are stacked in

TABLE 3

Technical Specifications of Aramid Kevlar29

Properties	Unit	
Type	# of filaments	1,000
Density	g/cm^3	1.44
Breaking Strength	N	338
Tensile Modulus	MPa	70,500
Elongation at Break	%	3.6
Tensile Strength	MPa	3,600

TABLE 4

Properties of Graphene Nanoplatelet (Nanografi, Türkiye)

Properties	Unit	
Purity	%	99.9
Size	nm	5
Diameter	µm	7
Surface Area	m^2/g	135
Conductivity	s/m	1100-1600
Colour	—	Gray

TABLE 5

Properties of Epoxy Resin (Verpol Brand, Türkiye)

Properties	Unit	A Component	B Component	Mixture
Viscosity	Brookfield (mPa·s)	1000-1250	40-70	250-350
Density	g/cm^3	1.15	0.95	1.09
Mixing Ratio	(w/w)	100	45	100/45
Colour	—	transparent	transparent	transparent
Pot Life	min	600		
Gel Time	Min	750		
Full curing	day	7 days @22°C		

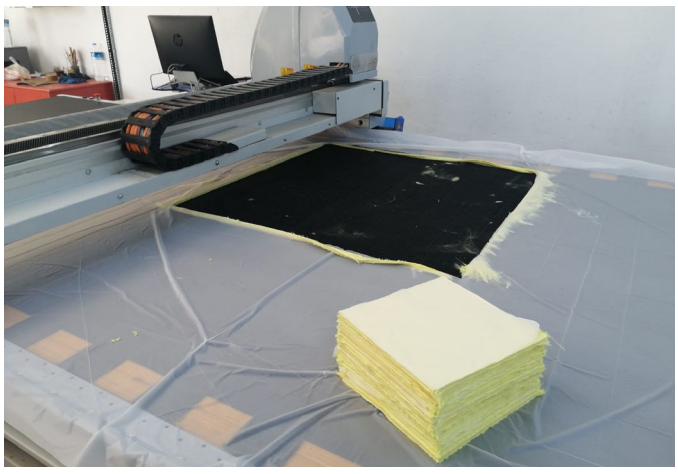

Fig. 3. Cutting of Aramid Layers

13 layers for plate formation. The weight of one aramid layer was measured at 27 g.

Many analysts have studied the influence of incorporation of various nano-fillers (graphene, carbon nanotubes, nanoparticles, nanomaterials and nanocellulose) in the range of 0.01 to 5 wt.% on the mechanical properties of fiber reinforced polymer nanocomposites. [9] Within this scope to determine the optimum amount of graphene additive, 0.5%, 1% and 1.5% by weight graphene additive was prepared (TABLE 6). The prepared graphene nanolayers together with epoxy resin, were mixed in a glass beaker with a manual mixer until a homogeneous structure was obtained. This mixture obtained was applied to these surfaces. This process has been applied to three layers of 13-layer plates and this process is shown in Fig. 4.

Fig. 4. Application of graphene nanopowder and epoxy resin

TABLE 6

Nomenclature of samples

Number	Ballistic Plate	Additive Status
1-2-3	13 Layer Kevlar 25×25 cm	No additive
4-5-6		0,5% Graphene ve Epoxy resin
7-8-9		1% Graphene ve Epoxy resin

The last stage is the pressing process of ballistic plates. After the graphene and epoxy resin mixtures were applied, the stacked layers were turned into ballistic plates under 135-145°C temperature and 15,6 N/mm^2 pressure values by pressing in hydraulic press. For mechanical and ballistic test processes, plates produced with 0.5, 1, and 1.5 weight percent graphene reinforced as well as plain aramid laminated plates are shown in Fig. 5.

To assess the properties of the materials, various tests were conducted, including Fourier Transform Infrared Spectroscopy (FTIR) for chemical characterization, Raman Spectroscopy for structural analysis, and Scanning Electron Microscopy (SEM) to examine surface morphology. For mechanical evaluation, tensile tests were performed using a Shimadzu tensile testing machine.

The ballistic performance was assessed following the NIJ-STD-0101.04 standard, where shooting tests were conducted using 9mm FMJ bullets at a distance of 5 meters. The impact areas were analyzed using digital imaging to examine penetration, fiber breakage, and energy dissipation mechanisms

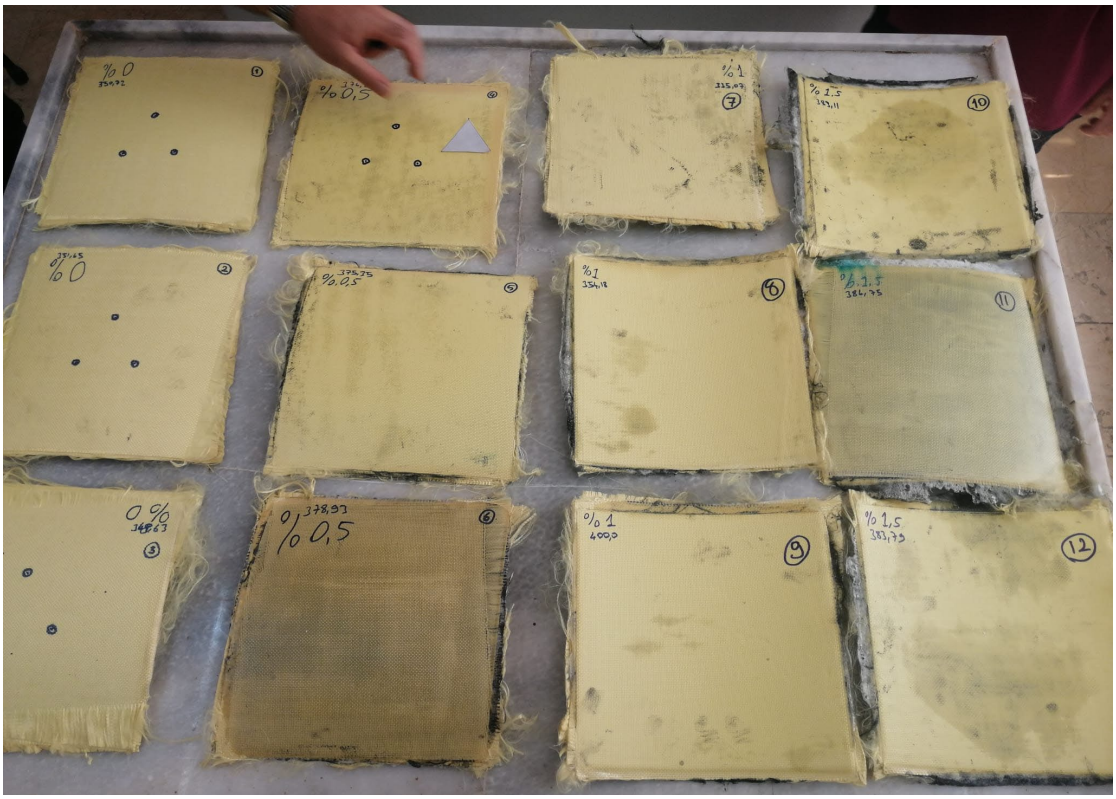

Fig. 5. Ballistic plates

2.3. FTIR analysis

Fourier transform infrared (FTIR) analysis of graphene used in the experimental study was performed by Perkin Elmer Spectrum UATR Two. Fourier transform infrared (FTIR) spectroscopy is a type of vibrational spectroscopy and is one of the most widely used methods for material characterization. In this method, the vibration frequencies of different bond structures of molecules are found by using infrared rays and it is ensured to obtain structural and functional information arising from vibrations. FTIR analyses were performed on solid samples.

2.4. Raman spectroscopy

Raman spectroscopy was performed on the graphene used in the experimental study by Renishaw Invia Raman Microscope. Point, depth, different resolution mapping and 3-dimensional (volume scanning) analyses can be performed. Thanks to lasers with two different wavelengths, 532 nm and 785 nm, it allows different types of materials to be analyzed effectively. Raman spectroscopy is a method that uses the interaction of light with matter to obtain information about the structure and properties of a substance. Raman spectroscopy provides information about intramolecular and intermolecular vibrations and enables the identification of a substance. Raman spectroscopy is an excellent instrument for the characterization of the layer thickness of graphene. There are a limited number of methods that provide information about the structure of graphene varieties, and Raman spectroscopy is the leading one.

2.5. SEM analysis

The LEO 1430 VP model SEM device used in the study has a W (Tungsten) filament. The device has secondary electron, backscattered electron and X-ray (EDX- Energy Dispersive X-ray Spectroscopy) detectors. The device can perform qualitative and semi-quantitative elemental analyses on the image with point, line, area and mapping methods. GNP powders were analyzed with SEM at different magnifications without applying any coating process.

2.6. Shooting test

In all shooting test processes in this study, the NIJ-STD-0101.04 standard was taken as a reference and the shots were made in the ballistic test laboratory in accordance with the test criteria in this standard. At the NIJ-STD-0101.04 standard IIIA protection level, the value of the depression formed on the target should be a maximum of 44 mm or there should be no perforation in the target when shooting with a 9 mm bullet from a distance of 5 m to the target. In addition, at the IIIA protection level, the muzzle velocity of the bullet in the test setup should be 436±10 (m/s).

In accordance with the NIJ-STD-0101.04 standard; In order to measure the ballistic strength at IIIA level, 12 samples were shot from a distance of 5 meters with a 9 mm FMJ (Full Metal Jacket) Parabellum bullet, with 3 shots per sample. Ballistic test shots were made in the ballistic test laboratory at 22°C temperature and 55% relative humidity. Ballistic plates and their properties are shown in TABLE 7.

TABLE 7

NIJ Standard 0101.04 Ballistic Test Chart

Armor Type	Test Round	Test Bullet	Bullet Weight / Grain	Reference Velocity	Max. Backface Deformation
IIIA	1	9 mm FMJ RN	8.2 g/124 gr.	1430±30 ft/s (436±10 m/s)	1.73 in (44 mm)

2.7. Tensile test

The tensile test determines the elastic and plastic behavior of materials under static load by Shimadzu AGS-X Series Universal Testing Device (100 kN). The sample is cut in specific dimensions in accordance with the standards and placed between the jaws of the device. By moving one of the jaws at a constant speed, a variable amount of tensile force is applied to the test sample and elongation corresponding this force is recorded.

The samples formed as a result of the application of graphene nanolayers to aramid fabrics were also subjected to the tensile test to be evaluated in terms of mechanical properties, as seen in Fig. 6.

Fig. 6. Tensile test

Thus, 0.5%, 1% and 1.5% by weight graphene added samples will be evaluated in comparison with non-graphene added samples. Sections taken from ballistic plates for the tensile test are shown in Fig. 7.

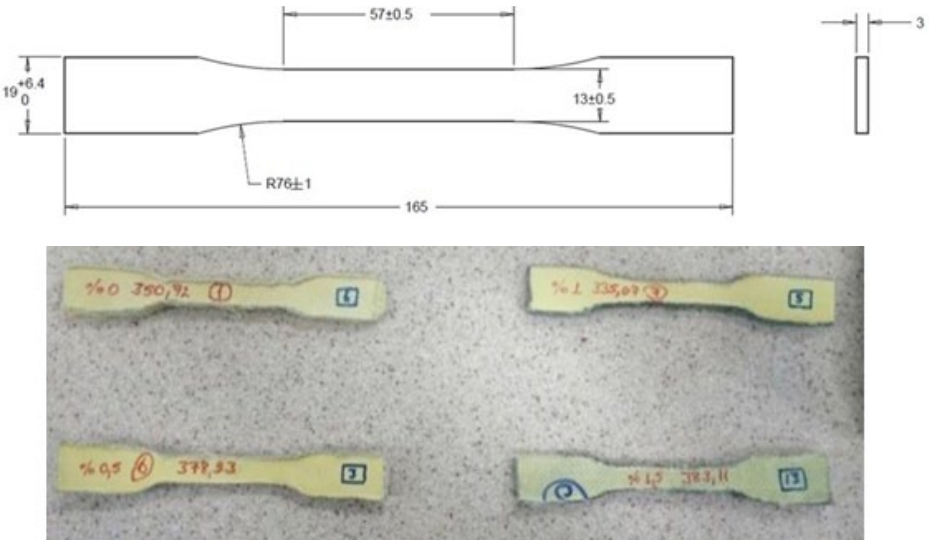

Fig.7. Samples of tensile test

3. Results and discussion

3.1. Results of FTIR analysis

According to results reported in the literature in the FTIR spectrum of graphene nanolayers; 1406 (C-H), 1068 (C-O), 886 and 610 (OH) cm^{-1} characteristic bands were obtained [20]. In the FTIR spectrum of the graphene nanolayers used in the experimental study in Fig. 8a. Fig. 8b presents the FTIR spectra of Aramid Kevlar 49. All three spectra exhibit four distinct peaks at 1653 cm^{-1} (amide C=O stretching), 1522 cm^{-1} (interaction between N-H stretching and bending), and 1313 cm^{-1} (coupling of C-N stretching with C-H bending) [21-23]. It was seen that the peak points were consistent with the values in the literature above. That shows an effective distribution of graphene throughout the composite matrix.

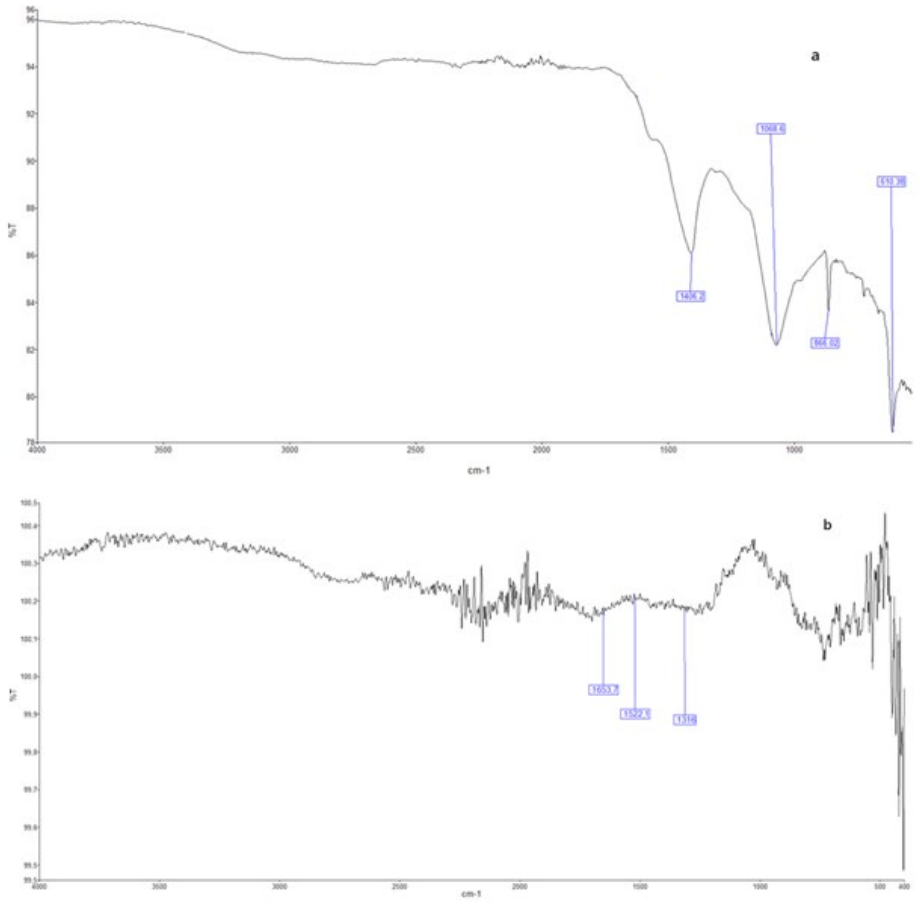

Fig. 8. FTIR spectrum of graphene(a) and aramid Kevlar29 (b)

3.2. Results of raman cpectroscopy

When using a 2.41 eV laser excitation target-monolayer graphene, Raman spectrum shows three major bands located at 1350 cm^{-1}, 1582 cm^{-1} (graphite) and 2700 cm^{-1} [24]. As can be seen in the Fig. 9, based on the Raman spectroscopy of the graphene used in the experimental study, peak points are in accordance with the literature above as well. Raman spectroscopy is a pivotal technique for characterizing graphene nanoplatelets (GNPs), providing insights into their structural integrity, defect density, and layer thickness. The primary features in the Raman spectrum of GNPs are the D, G, and 2D bands. The G band, located around 1580 cm^{-1}, corresponds to the E_2g phonon at the Brillouin zone center and is indicative of the sp^2 hybridized carbon networks. The D band, appearing near 1350 cm^{-1}, is associated with breathing modes of six-atom rings and requires a defect for its activation, thus serving as a marker for defects within the graphene structure. The 2D band, found approximately at 2700 cm^{-1}, is the second order of the D band and is sensitive to the number of graphene layers [25,26]

3.3. Images of SEM analysis

Scanning electron microscope (SEM) images of GNP are given in Fig. 10.

As seen in Fig.10, it is clear that GNP powders are in the form of layers. Clumps are also observed due to agglomeration caused by the moisture it absorbs.

3.4. Results of shooting tests

Graphene doped and undoped aramid plates were exposed shooting test in accordance with the test criteria specified in NIJ-STD-0101.04 standard IIIA protection level. Ballistic tests were carried out with a 9 mm diameter FMJ (Full Metal Jacket) bullet at a distance of 5 meter to the target. According to the standard, the criterion for success is that the value of the depression formed on the target is at most 44 mm or there is no perforation in the target. Ballistic test results on plates are given in TABLES 8-11.

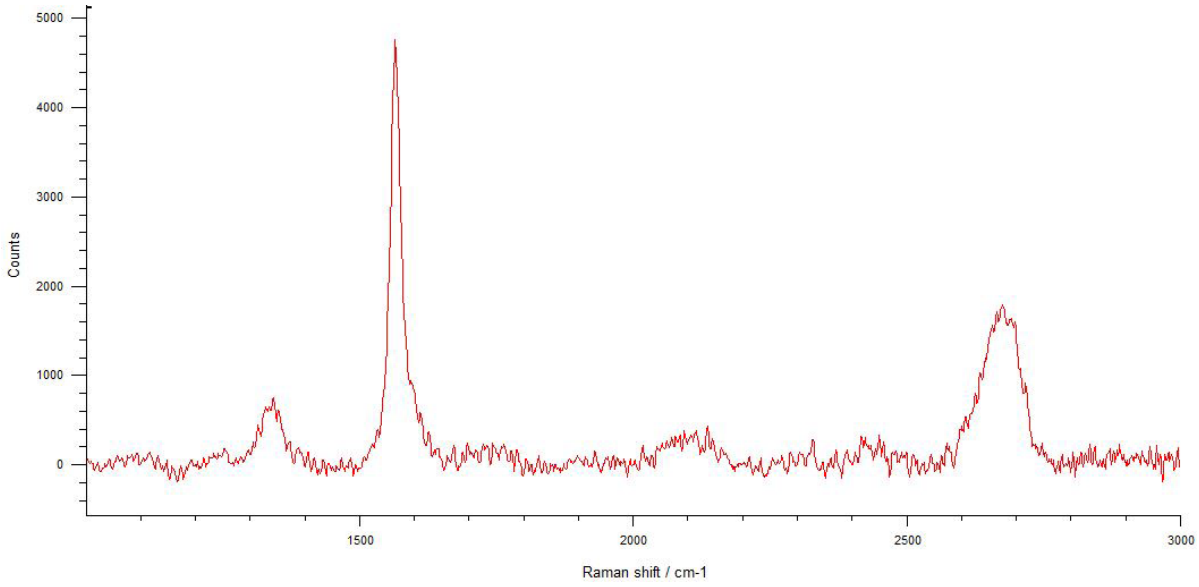

Fig. 9. Raman spectroscopy of graphene

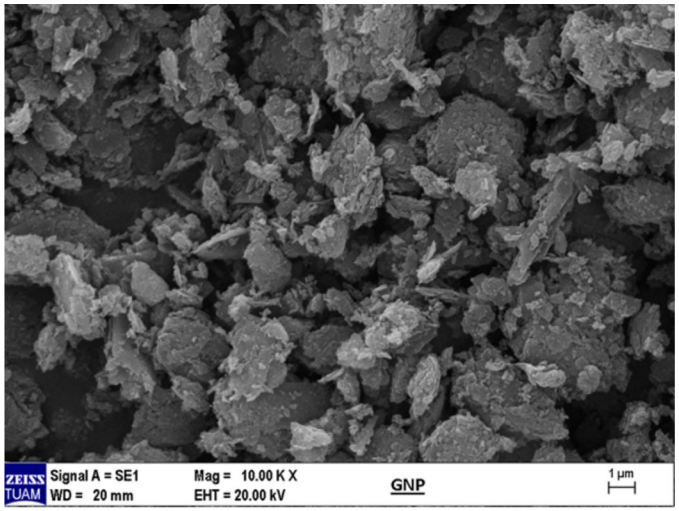

Fig. 10. SEM images of GNP

According to the results of the shooting test, plain kevlar layered plates met the ballistic protection criterion. However, perforation occurred in all but one of the graphene added plates. As a result, negative effects of graphene and epoxy resin additives on ballistic protection were observed.

Plates and bullets that were perforated as a result of shooting tests were examined. It has been observed that the aramid plates with graphene and epoxy resin added nanocomposite structure are harder and brittle than the plates without graphene and epoxy additives. It has been evaluated that this situation is caused by the penetration of epoxy resin into aramid fabrics during hot press-

TABLE 8

Shooting test result of plain kevlar plates

Number	Ballistic Plate	Type of Bullet	Number of Shooting	Velocity of Bullet (m/s)	Depth of Depression (mm)	N	Mean	StDev	95%CI
1	Only kevlar	9 mm FMJ	1	433	23	9	25,667	2,598	(20,750; 30,584)
			2	436	24				
			3	440	29				
2			1	441	28				
			2	438	23				
			3	436	25				
3			1	444	29				
			2	441	27				
			3	438	23				

TABLE 9

Shooting test result of 0,5% graphene added plates

Number	Ballistic Plate	Type of Bullet	Number of Shooting	Velocity of Bullet (m/s)	Depth of Depression (mm)	N	Mean	StDev	95%CI
4	0,5% graphene added	9 mm FMJ	1	439	Perforated	9	41,44	7,67	(36,53; 46,36)
			2	440	Perforated				
			3	426	21 mm				
5			1	438	Perforated				
			2	440	Perforated				
			3	441	Perforated				
6			1	429	Perforated				
			2	430	Perforated				
			3	445	Perforated				

TABLE 10

Shooting test result of 1% graphene added plates

Number	Ballistic Plate	Type of Bullet	Number of Shooting	Velocity of Bullet (m/s)	Depth of Depression (mm)	N	Mean	StDev	95%CI
7	1% graphene added	9 mm FMJ	1	438	Perforated	9	44,00	0,00	(39,08; 48,92)
			2	432	Perforated				
			3	430	Perforated				
8			1	428	Perforated				
			2	426	Perforated				
			3	430	Perforated				
9			1	429	Perforated				
			2	441	Perforated				
			3	430	Perforated				

TABLE 11

Shooting test result of 1.5% graphene added plates

Number	Ballistic Plate	Type of Bullet	Number of Shooting	Velocity of Bullet (m/s)	Depth of Depression (mm)	N	Mean	StDev	95%CI
10	1.5% graphene added	9 mm FMJ	1	436	Perforated	9	36,00	12,01	(31,08; 40,92)
			2	438	Perforated				
			3	442	Perforated				
11			1	426	Perforated				
			2	438	Perforated				
			3	430	Perforated				
12			1	440	21				
			2	428	20				
			3	445	Perforated				

ing. In other words, the epoxy resin made the flexible structure of the aramid brittle and reduced the kinetic energy absorption capacity of the aramid fibers. The plates, which became harder and brittle, could not absorb the kinetic energy of the bullet and caused perforation (Figs. 11-12).

When the projectiles used after shooting were examined, it was observed that only the bullets used in aramid plates kept their integrity, while the bullets used in graphene and epoxy resin plates were fragmented. In other words, the plates in question could not stop the bullet, but damaged the physical structure of the projectile.

The method of spreading the selected nanomaterial on the composite plate affects the ballistic performance. Homogeneous distribution of the nanomaterial on the composite plate will improve the mechanical and ballistic properties of the plate. In addition to the hand lay-up method used in this study, it is evaluated that using different methods such as vacuum assisted resin transfer, vacuum assisted manual laying will provide high quality samples.

Though very few in numbers, there are studies present in literature where nanoparticles have been found to improve projectile penetration into the composites. For example, Avila et al. In another study [27], impact performance under ballistic condition of glass/epoxy composites was studied in details. This study was based on the incorporation of nanoclay and nanographite on the ballistic performances of the composite. The fact that the high-speed impact performance of glass/epoxy composites is strongly influenced in terms of failure modes by the incorporation of nanoclay and graphene nanolayers in glass/epoxy composites has been established. In nanocomposites, besides

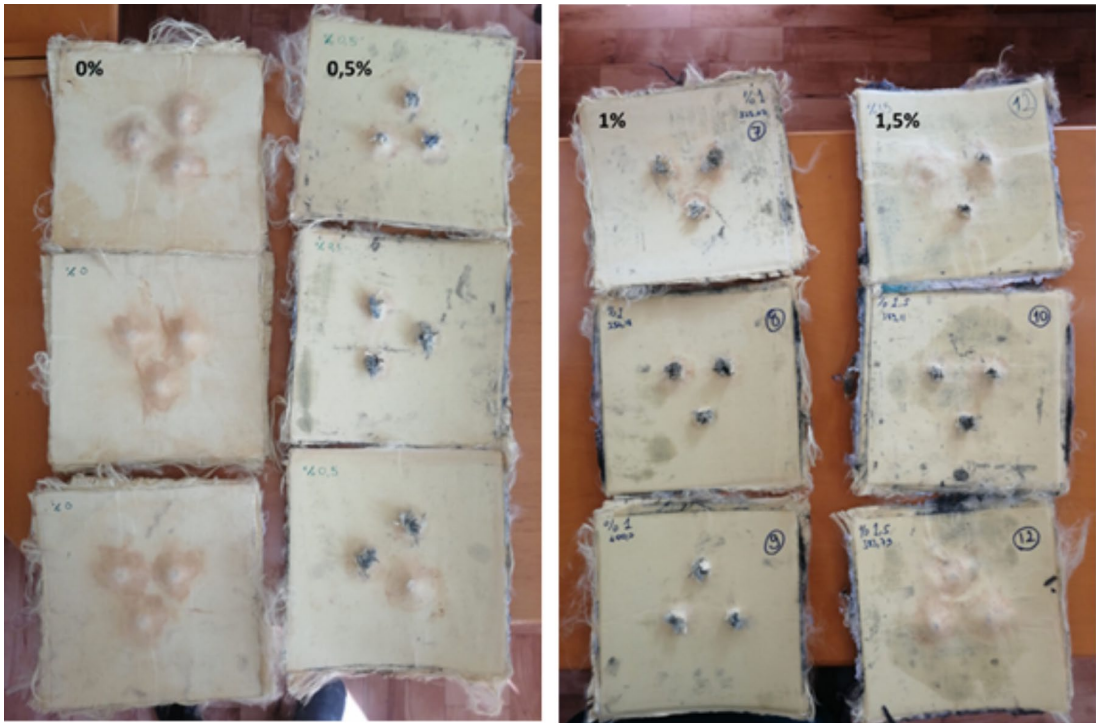

Fig. 11. Micro images of the deformation regions of ballistic plates

Bullet entry point | Bullet penetration point | Backface deformation

Fig. 12. Movement of bullet on ballistic plates

the component types, the weight ratio of the nanoparticles and the distribution patterns in the matrix are key factors to obtain the desired properties.

In another study, Gibson et al. [28] tested various armor composite panels consisting of Kevlar 29 fabric with added carbon nanotubes and/or carbon fibers in an epoxy matrix under different ballistic impact conditions. For the combination of 1.65% carbon nanotube and 1.65% fiber by weight, detected a 6.5% improvement in the V50 ballistic test results.

3.5. Results of tensile test

Tensile tests were performed on 4 different samples with no graphene additive and 0.5%, 1% and 1.5% graphene additives by weight, and the stress and strain graphs of the said samples are examined and calculated ultimate tensile strength (UTS). Ultimate tensile strength (UTS) is defined as the maximum engineering stress level reached in a tensile test, that is, the level of ability of a material to withstand external forces without breaking. UTSs determined in the graphics above are shown in TABLE 12. Looking at the values below, it is seen that the graphene additive increases the tensile strength of the aramid sample at 0.5% and 1% by weight, but decreases the tensile strength at 1.5% by weight.

TABLE 12

Ultimate tensile strength of samples

Number	Percentage of graphene additive (%)	UTS (MPa)
1	No	147
2	0,5	172
3	1	270
4	1,5	108

As a result of the tensile tests, it was determined that 0.5% and 1% by weight graphene additive increased the ultimate tensile strength of the aramid plate and improved its mechanical properties. In comparison with graphene-free samples; UTS increased by 21% with 0.5% by weight graphene additive and 84% with 1% by weight graphene additive. However, UTS decreased by 27% at the 1.5% by weight graphene additive. As a result, it should not be forgotten that determining the optimum amount of nanomaterials as reinforcement material in composites is an important criterion affecting the mechanical properties of the composite.

4. Conclusions

The rapid advancements in ballistic and weapon technologies necessitate continuous improvements in armor design and materials. This study investigated the effect of graphene reinforcement on the ballistic and mechanical performance of aramid-based composite plates. While graphene has been widely recognized for its exceptional mechanical properties, its application in ballistic protection requires further optimization.

The experimental results demonstrated that plain Kevlar-based ballistic plates met the NIJ-STD-0101.04 ballistic protection criteria, while graphene-reinforced plates, except for one case, failed to prevent perforation. This outcome suggests that the addition of graphene and epoxy resin altered the structural properties of the aramid layers, making them more rigid and brittle, which negatively affected their energy absorption capacity. The interaction between epoxy resin and aramid fibers played a crucial role in reducing the effectiveness of graphene as a reinforcement material for ballistic protection.

On the other hand, mechanical tests revealed that adding 0.5% and 1% by weight of graphene to the composite significantly improved the ultimate tensile strength of the plates, increasing it by 21% and 84%, respectively, compared to the non-reinforced samples. However, at 1.5% graphene content, the tensile strength decreased, highlighting the importance of determining the optimal graphene concentration to achieve desired mechanical properties without compromising flexibility.

These findings indicate that while graphene has the potential to enhance certain mechanical characteristics of ballistic composites, further research is required to refine its application in armor design. Future studies should focus on alternative dispersion methods, different graphene integration techniques, and the potential combination of graphene with other reinforcement materials to maximize ballistic performance. The development of innovative nanocomposite manufacturing approaches could lead to the creation of lightweight, highly durable, and more effective personal protective armor solutions.

Acknowledgements

This study was supported by Afyon Kocatepe University Scientific Research Projects Coordination Unit (AKÜ BAPK, Project Number: 20.FEN.BIL.29). A preliminary version of this research was presented at the International Symposium on Characterization, ISC'22.

REFERENCES

[1] M. Fakruddin, Z. Hossain, H. Afroz, J. Nanobiotechnol. **10**, 31 (2012). DOI: https://doi.org/10.1186/1477-3155-10-31

[2] A. Vlandis, Chain Reaction **97**, 27-28 (2006).

[3] P.M. Cunniff, Text. Res. J. **62** (9), 495-509 (1992). DOI: https://doi.org/10.1177/004051759206200902

[4] P.J. Hogg, Science **314** (5802), 1100-1101 (2006). DOI: https://doi.org/10.1126/science.1131118

[5] G. Thilagavathi, A.S.M. Raja, T. Kannaian, Def. Sci. J. **58** (4), 451-459 (2008). DOI: https://doi.org/10.14429/dsj.58.1667

[6] L. Wang, S. Kanesalingam, R. Nayak, R. Padhye, Text. Light Ind. Sci. Technol. **3**, 37-47 (2014). DOI: https://doi.org/10.14355/tlist.2014.03.007

[7] M. Jacobs, J. Van, J. Mater. Sci. **36**, 3137-3142 (2001). DOI: https://doi.org/10.1023/A:1017922000090

[8] M. Dobb, R. Robson, J. Mater. Sci. **25**, 459-464 (1990). DOI: https://doi.org/10.1007/BF00714056

[9] N.M. Nurazzi, M.R.M. Asyraf, A. Khalina, N. Abdullah, H.A. Aisyah, S.A. Rafiqah, Polymers **13** (4), 1-42 (2021). DOI: https://doi.org/10.3390/polym13040646

[10] K.S. Novoselov, A.K. Geim, S.V. Morozov, D. Jiang, Y. Zhang, S.V. Dubonos, et al., Science **306** (5696), 666-669 (2004). DOI: https://doi.org/10.1126/science.1102896

[11] A.S. Wajid, S. Das, F. Irin, H.T. Ahmed, J.L. Shelburne, D. Parviz, et al., Carbon **50**, 526-534 (2011). DOI: https://doi.org/10.1016/j.carbon.2011.09.008

[12] K. Liew, Z. Lei, L. Zhang, Compos. Struct. **120**, 90-97 (2015). DOI: https://doi.org/10.1016/j.compstruct.2014.09.041

[13] J.H. Lee, P.E. Loya, J. Lou, E.L. Thomas, Science **346** (6213), 346 (2014). DOI: https://doi.org/10.1126/science.1258544

[14] A.C. Pereira, A.M. Lima, L.C.D.C. Demosthenes, M.S. Oliveira, U.O. Costa, W.B.A. Bezerra, et al., Polymers **12** (11) (2020). DOI: https://doi.org/10.3390/polym12112711

[15] F. Bozdoğan, S. Üngün, E. Temel, G. Süpüren Mengüç, Tekstil ve Mühendis **22** (98), 84-103 (2015). DOI: https://doi.org/10.7216/130075992015229808

[16] NIJ-STD-0101.04, U.S. Department of Justice Office of Justice Programs National Institute of Justice, USA, 2001.

[17] R. Scott, Textiles for Protection, Cambridge, Woodhead Publishing, 2005.

[18] P.V. Cavallaro, Newport, USA, Tech. Report, NUWC-NPT 12,057, 1 August 2011.

[19] G. Cooper, P. Gotts, Ballistic protection in Ballistic Trauma, Springer, 67-90 (2005). DOI: https://doi.org/10.1063/5.0068916

[20] Y. Gong, D. Li, Q. Fu, C. Pan, Prog. Nat. Sci. Mater. **25**, 379-385 (2015). DOI: https://doi.org/10.1016/j.pnsc.2015.10.004

[21] I. Mohamad, H. Hussein, J. Rafi, Revue des composites et des matériaux avancés **30** (2020). DOI: https://doi.org/10.18280/rcma.303-403

[22] J. Zhao, Fibers Polym. **14** (1), 59-64 (2013). DOI: https://doi.org/10.1007/s12221-013-0059-x

[23] H.J. Kong, H. Sun, J. Chai, H.Q. Ding, X.M. Ding, M.M. Qiao, M.H. Yu, Y.F. Zhang, Polym. Compos. **40** (S1), E920-E927 (2019). DOI: https://doi.org/10.1002/pc.25100

[24] L. Malard, M.A. Pimenta, G. Dresselhaus, M. Dresselhaus, Phys. Rep. **473** (5), 51-87 (2009). DOI: https://doi.org/10.1016/j.physrep.2009.02.003

[25] J. Patel, A. Kiani, Tribological Behaviours of Different Base Greases Enhanced by Graphene Nano Platelets, 2019. DOI: https://doi.org/10.11159/tann19.140

[26] R.H. Bello, L.A.F. Coelho, D. Becker, J. Compos. Mater. (2017). DOI: https://doi.org/10.1177/0021998317709082

[27] A.F. Avila, A.S. Neto, H.N. Junior, Int. J. Impact Eng. **38** (8), 669-676 (2011). DOI: https://doi.org/10.1016/j.ijimpeng.2011.03.002

[28] J. Gibson, J. McKee, G. Freihofer, S. Raghavan, J. Gou, Int. J. Smart Nano Mater. **4**, 212-228 (2013). DOI: https://doi.org/10.1080/19475411.2013.870938